IOSR Journal Of Applied Physics (IOSR-JAP)
e-ISSN: 2278-4861.Volume 15, Issue 2 Ser. I (Mar. – Apr. 2023), PP 21-27
www.Iosrjournals.Org

Studies the various property of strontium stannate prepared by coprecipitation method

Rakesh Kumar Kurre
Department of Physics,
Govt. J. M. P. College Takhatpur , Bilaspur (Chhattisgarh)

Abstract:
The compound $SrSnO_3$ belongs to the family of analogous alkaline-earth stannates $MSnO_3$ (where M=Ca, Sr and Ba) which is widely investigated for their attractive dielectric and electronic properties. It is important for ceramic and electronic industry where they can be used as thermally stable capacitors and gas sensors. The main interest of our research work is to prepared strontium stannate by a novel chemical Co-precipitation route. Crystal structure was characterized using x-ray diffraction (XRD) pattern which show the formation of single phase materials having orthorhombic perovskite structure. Temperature and frequency dependence dielectric constant and loss was measured in temperature range from room temperature up to 300 ^0C which shows highly thermally stable and low loss materials. The SEM micrographs are showing fine grains for the sample.

Keywords: *X-ray diffraction, dielectric spectroscopy, electrical characterization, impedance analysis.*

Date of Submission: 09-03-2023 Date of Acceptance: 22-03-2023

I. Introduction:

Recently stannates $MSnO_3$ (M=Sr, Ca, Ba) as a component of dielectric materials have received much attention due to their applications as thermally stable capacitors in electronic industries [1] and gas sensors[2,3]. Strontium, stannate, $SrSnO_3$, has been reported to be used in humidity sensors [4]. Solid solutions of alkaline earth titanates and stannates are also used for the fabrication of ceramic boundary layer capacitors [5]. Strontium stannate ($SrSnO_3$) are most important technically and industrially interesting ceramics. It is dielectric material for technological importance and also used as semiconductor sensors for humidity and gases. $SrSnO_3$ is normally synthesized at temperatures above 1000 ^{0}C by solid state reaction between $SrCO_3$ or SrO and SnO_2. The relatively high preparation leads often to powders of large and varied grain sizes and varying impurity content. The stannates have already been synthesized successfully using different methods, like as high temperature solid state reaction of mixtures of $M(NO_3)_2/SnO_2$ or MCO_3/ SnO_2 powders at 1000-1200 ^{0}C for $SrSnO_3$ [6-8] and at 1000-1450 ^{0}C for other stannates [9-11]. Apart from these ceramic routed those stannates can also be prepared by sol-gel techniques [12] or the thermal decomposition of oxalates [13]. Despite the many syntheses and characterization of strontium stannate ($SrSnO_3$) which have frequently been under investigation in the literature, low temperature and short time syntheses methods are rare [14-15]. All above mentioned ceramics routes for the preparation of the stannates have in common long synthesis times (up to 16 h).Therefore an low cost synthesis route using shorter times and lower temperatures are clearly demanded.

We hereby report a synthesis of strontium stannate by using co-precipitation method at significantly low temperature and shorter reaction times. In this paper we present the result of XRD, SEM, dielectric, impedance, AC & DC Conductivity measurement of strontium stannate.

II. Experimental:

Aqueous solutions of Strontium chloride $SrCl_2$ $6H_2O$ and Tin chloride $SnCl_4$ $5H_2O$ were used as starting materials. The concentrations of the Ba^{2+} and Sn^{4+} solutions were about 0.2 and 0.3 M, respectively. The concentration of the aqueous oxalic acid used as the precipitant was about 0.12 M. Stoichiometric amounts of Sr^{2+} and Sn^{4+} solutions were mixed and then the aqueous $(CHOOH)_2$ $.2H_2O$ oxalic acid was slowly added to the mixed solution. White oxalate precipitates were prepared and then stirred for 2h. The oxalate precipitates after aging for 2h were filtered and then washed by ethanol. The Oxalate precipitates were dried at 110 ^{0}C for overnight. $SrSnO_3$ powder was prepared by calcinations of the dried oxalate precipitates at 1050 ^{0}C for 3 h and sintered at 1100 ^{0} C for 4 h. Strontium Stannate powder are confirmed by X-ray diffractometer (Rigaku). These were pressed as cylindrical pellets (dia 10 mm and 1-2 mm thickness) after adding a few drops of poly vinyl alcohol as binder.

Finally the pallets were kept in furnace at 1100 ^{0}C for 4hrs for completing sintering process. After firing the samples were furnace cooled. The pellets were finally coated with conductive silver paint and dried at 400 ^{0}C for 2 hrs before taking dielectric and impedance measurement. X ray diffraction and AC conductivity for this pellet was measured using. The percentage porosity was calculated from there experimental density (Archimedes principle) and theoretical density. X-ray diffraction (XRD) studies of the materials were measured at room temperature in the Bragg angle range $20 \leq 2\theta \leq 60$ ^{0}C by an X-ray diffractometer (Rigaku miniflex, japan) CuKα radiation (λ= 1.5418 Å). The dielectric constant and impedance were measured over temperature range from 30-300 ^{0}C using a Computer controlled impedance analyzer (HIOKI LCR Hi-TESTER MODEL 3532-50) in the frequency range 1 kHz to 1 MHz AC and DC conductivity were studied for this sample. For these purpose we used keithley LCR meter. The complete processes of material preparation are displayed by flowcharts.

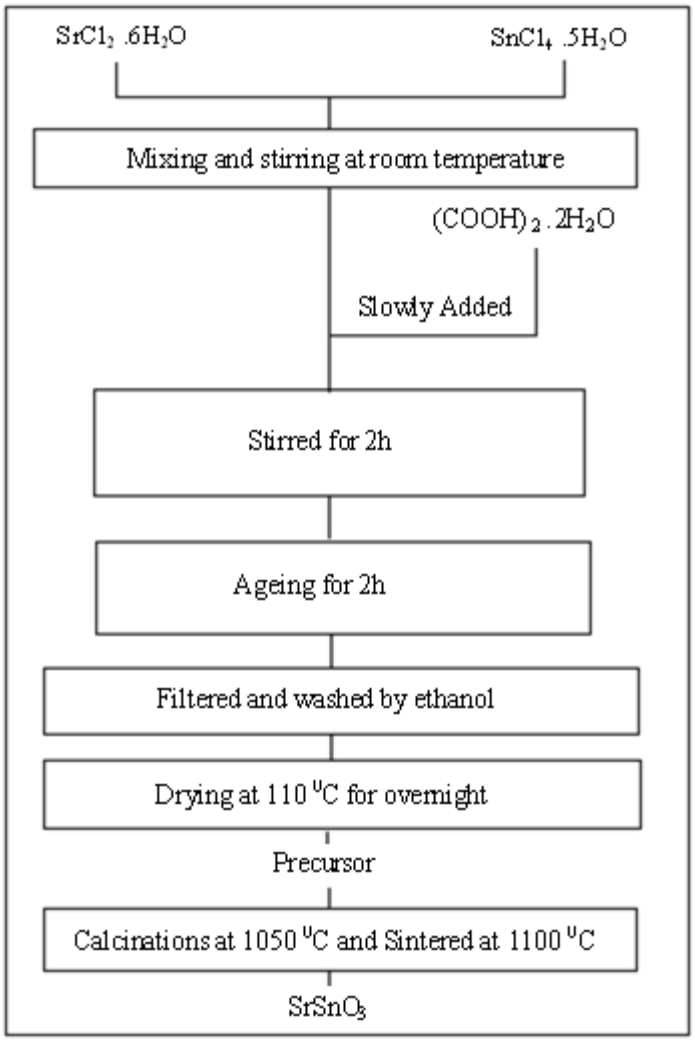

FLOWCHART OF EXPERIMENTAL TECHNIQUE

III. Result And Discussion:

XRD- The oxalic acid has been used as the precipitant for the preparation of $BaTiO_3$ Barium titanate powders by the coprecipitation method of the mixed solution of Ba^{2+} and $Ti^{4+.}$ The similar method was applied to the preparation of the $SrSnO_3$ powders. The white precipitates were prepared by the addition of the aqueous oxalic acid to the mixed solution of Sr^{2+} and Sn^{4+}. The resulting powers were identified from x-ray powder diffraction patterns recorded at higher temperature with a X-ray diffractometer (Rigaku miniflex, japan) CuKα radiation (= 1.5418 Å). The X-ray powder diffraction pattern of the final product is shown in Fig. 1.

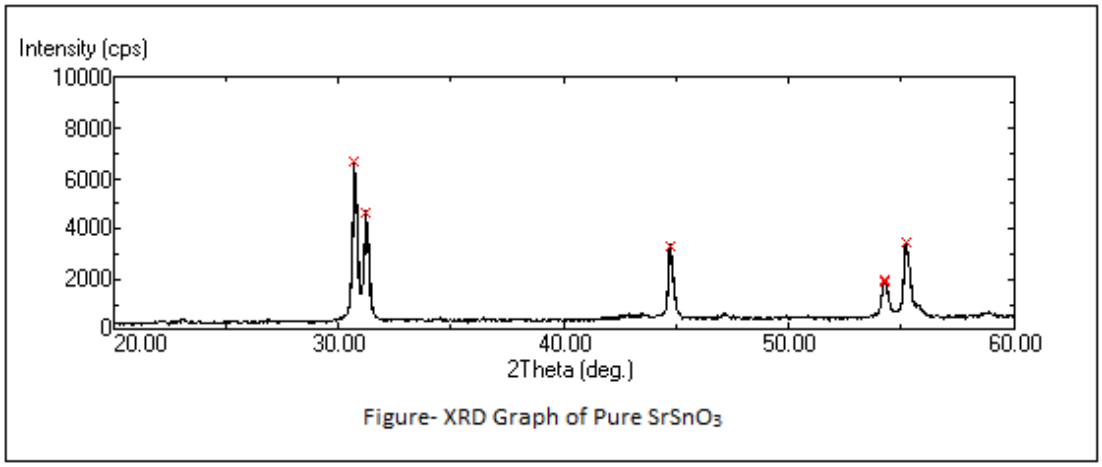

Figure: 1 XRD Pattern of Pure $SrSnO_3$

This is indicating that the compound was identified as an orthorhombic- like phase. X-ray diffraction patterns could be indexed on the basis of an orthorhombic unit cell and JCPDF No. 77-1798. We have report the lattice parameters of the sample is a=5.7356A, b=5.7448, c=8.3881 shows Table 1[a] .All the diffraction peaks can be indexed to the orthorhombic structure without any impurity phase. The phase formation of the sample was selected according the good agreement between observed and calculated d-values. The d-observed value (d_{obs}) and d-calculated value (d_{cal}) was well matched having minimum standard deviation in the orthorhombic crystal system. Measured experimental density of the sample is 91.2% for pure strontium Stannate. The crystallite size of the samples was calculated from the peak width and peak position of the reflections using Debey-Scherrer relation .the values are given in table 1[b].

Pure $SrSnO_3$ a= 5.7356 ,b= 5.7448 c= 8.3881 v= 276.38 , SD=.00080 A					
D value		Intensity	Indices		
Obs.	Cal.		h	k	l
2.9151	2.9167	100	1	1	2
2.8678	2.8678	70	2	0	0
2.0297	2.0295	50	2	2	0
1.6939	1.6937	30	0	2	4
1..6667	1.6668	52	1	3	2

Table -1[a] Variation of lattice parameters.

Structure	Composition	Theoretical Density (gm/cm^3)	Experimental Density (gm/cm^3)	Density %
Orthorhombic	Pure $SrSnO_3$	7.6388	6.9689	91.2%

Table- 1[b] Density Measurement

Dielectric studies-The figure 2 (a) & (b) shows the variation of for dielectric constant and dielectric loss vs. temperature at 1 kHz, 5 kHz, 10 kHz,50 kHz,100,500 kHz, and 1000 kHz for pure $SrSnO_3$ by co-precipitation method. From these plots, it is observed that both ε' and tan δ almost thermally stable. It is observed that the dielectric constant increases slightly with temperature. This type of dielectric behaviour of the sample indicates almost negligible contribution from interfacial and space charge polarization. The dielectric loss is almost 1% of the dielectric constant support the thermal stability of the materials.

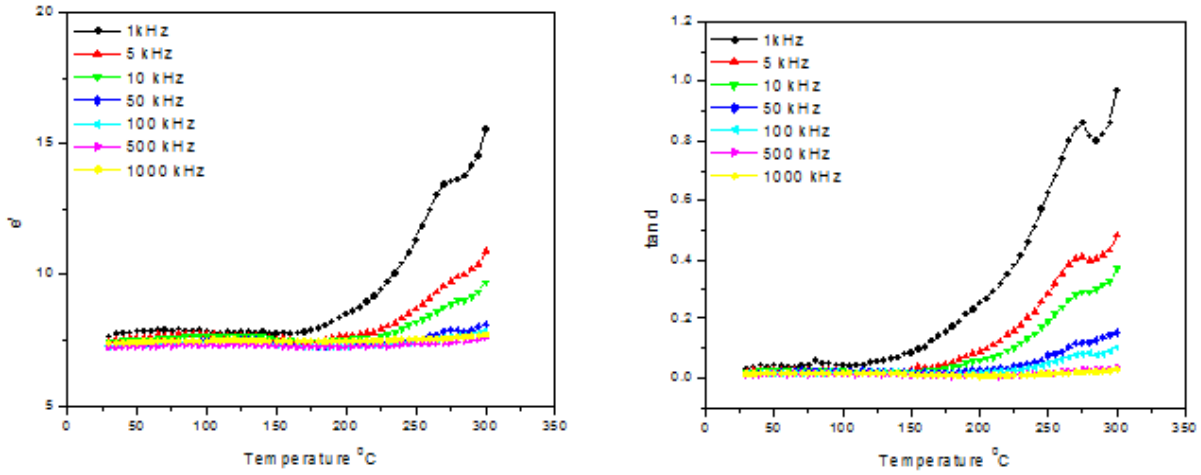

Figure 2(a) & (b): Dielectric constant & loss Vs Temperature.

The variation of dielectric constant and tangent loss as function of frequency at different temperature. it is indicate the dielectric constant and loss were slightly decreased with the temperature that means perform a low frequency dielectric dispersion at selected frequency. In this result the value of dielectric constant increases on different temperature for this sample. This result may be attributed to combined contribution to a dielectric constant due to electronic, ionic, interfacial polarization at low frequencies. The tangent loss was maximums at lower frequency for different temperature. The loss spectra indicate that the sample behaviour is thermally activated at high temperature. This is due to the presence of space charge polarization. Shows the figure 3(a) & (b)

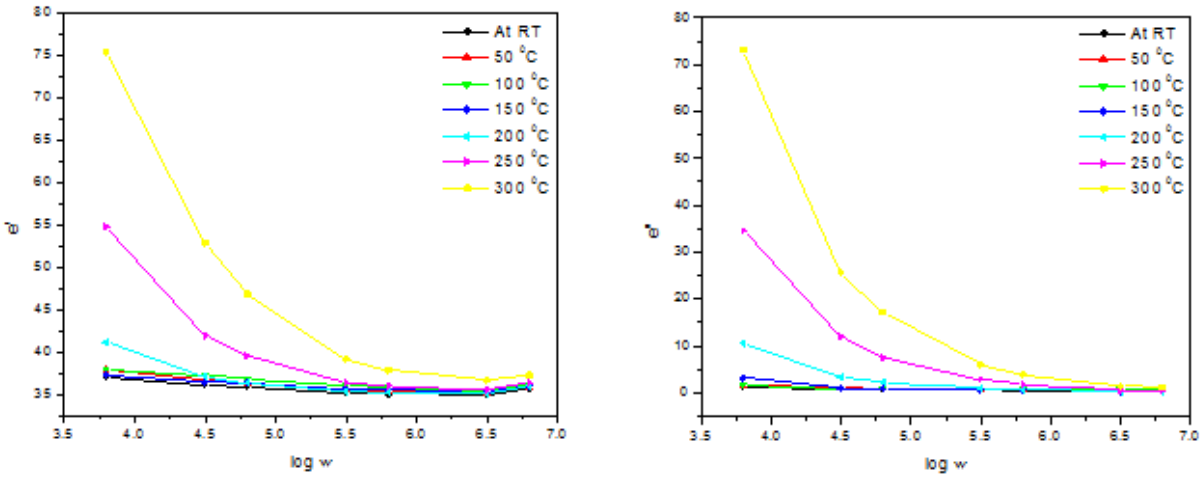

Figure 3(a) & (b): Dielectric constant & loss Vs Frequency.

Impedance-In order to complete understanding of electrical conduction mechanism, it is essential to distinguish the grain and grain boundary effects in the material matrix at that particular temperature and frequency domain. For this purpose we have employed complex impedance and modulus analysis. Impedance and modulus analysis are frequently used for analysis of the electrical conductivity of the materials. The Variation of real part of impedance (Z') and imaginary part (Z'') as a function of frequency is shown for different temperature range room temperature up to 300 ^{0}C Figure 4(a) & (b). From impedance plots, it is observed that value of Z', and Z'' decreases with frequency at all temperatures. This indicates that dispersion in values of Z' and Z'' is high at lower frequency. Value of Z' and Z'' are almost invariant with frequency at all measured temperature of the sample. Although dispersion in the imaginary part of impedance Z'' verses frequency is less comparison to real part of impedance verses frequency plots.

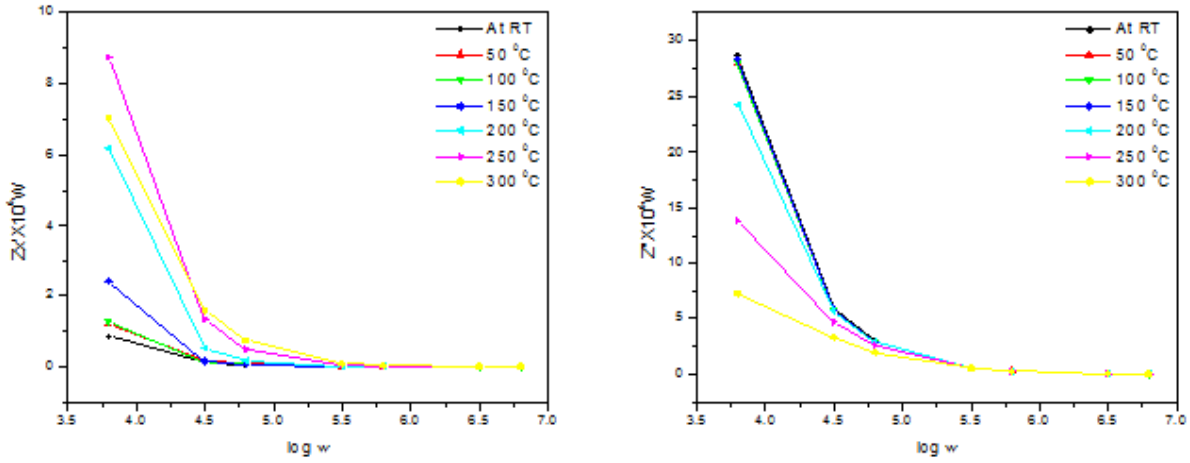

Figure 4(a) & (b): Real and imaginary part of impedance.

AC Conductivity-The variation a.c. conductivity as a function of frequency and temperature is shown in figure 5(a) & (b).The a.c. conductivity (σ_{ac}) of the system depends on the dielectric properties and sample capacitance of the material. The nature of variation of the σ_{ac} for $SrSnO_3$ indicates the conductivity dispersion throughout the range of frequency under investigation. This behaviour may be attributed to the presence of space charge in the material. The ac conductivity was calculated from the impedance data using the relation $\sigma_{ac} = \omega\varepsilon_0\varepsilon_r(\tan\delta)$. It is clear from the figure that the materials at low frequencies exhibit dispersion. The temperature at which the grain resistance dominates over grain boundary is marked by change in slope of conductivity with frequency. The electrical conductivity in the different regions of the frequency changes which may be due to the hopping of conducting charge species and polarons in both short and long range ordering.

Temperature dependent conductivity data shows the linear behaviour of conduction in low temperature region ($T \leq 200\ ^0C$) and non-linear conduction behaviour in the high temperature region which well obeys the Arrhenius type thermally activated conduction process. The conductivity of the material at is found to increase with increase in temperature indicating the NTCR (negative temperature coefficient of resistance) like semiconductors.

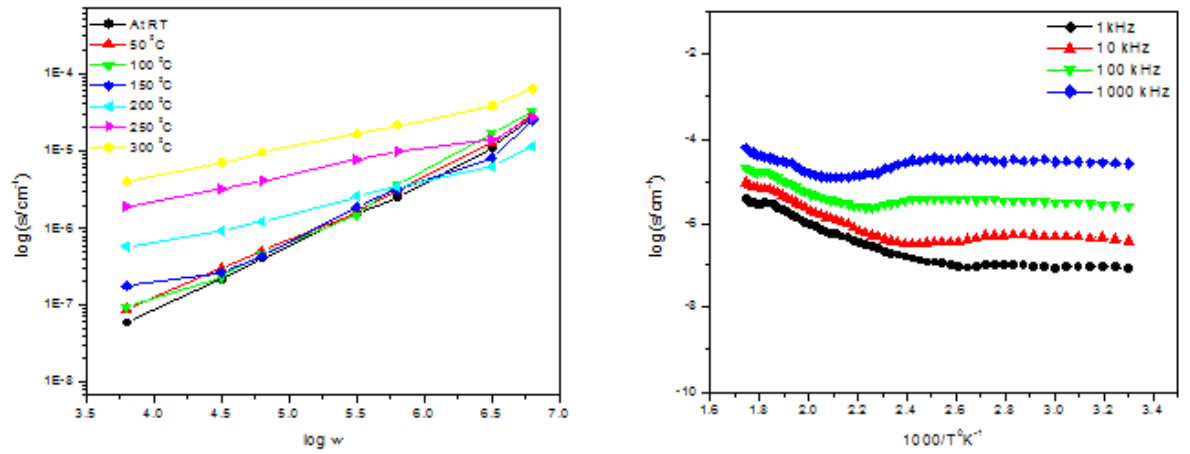

Figure 5 (a) & (b): AC Conductivity Vs Frequency & Temperature.

DC Conductivity- Plots of log σ_{dc} vs 1000/T for this sample are shown in figure. (6) shows the variation of d.c. conductivity as a function of temperature. The nature of variations suggests that d.c. conductivity decreasing with increase of temperature. The rise in conductivity may be due to thermally generated carriers in the sample. A change in the slope of the Arrhenius plots was observed. It is reported that slight change in slope is related to transition temperatures (Prasad 2000).The slight change in slopes may be due to contribution from different regions in polycrystalline materials (i.e. from grain, grain boundary etc).

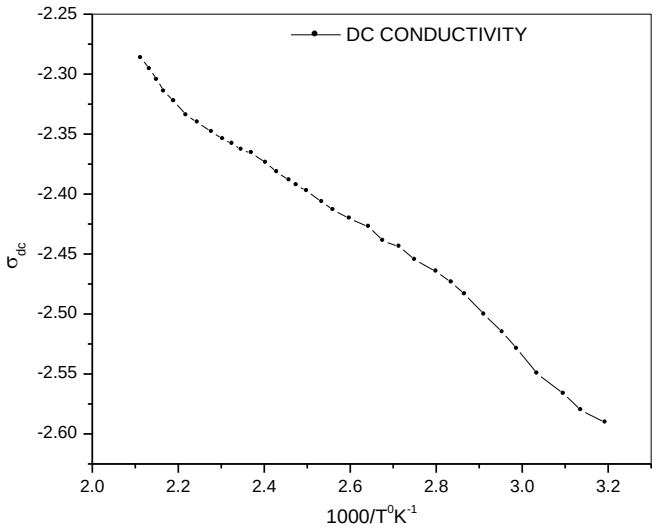

Figure 6: DC Conductivity Vs Frequency & Temperature.

SEM-The surface morphologies precursor material $SrSnO_3$ was studied by scanning electron microscopy (Zeiss EV 6). The microstructure is a very important factor which most be controlled during the elaboration of the powder. The SEM was used to examine microstructure and chemical feature of the prepared sample. The microstructure was analyzed by scanning electron microscopy which is almost spherical shape. The SEM micrographs of samples are shown in figure 7(a) & (b)

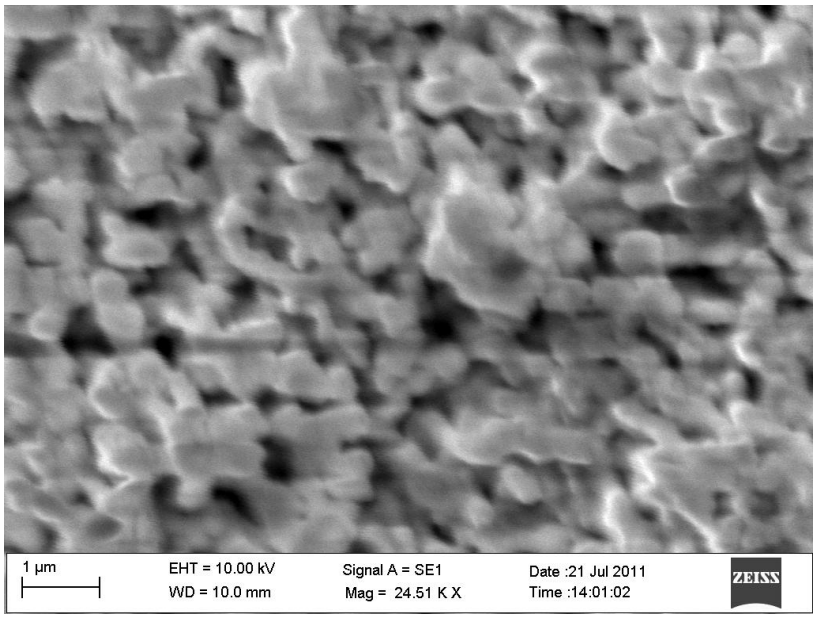

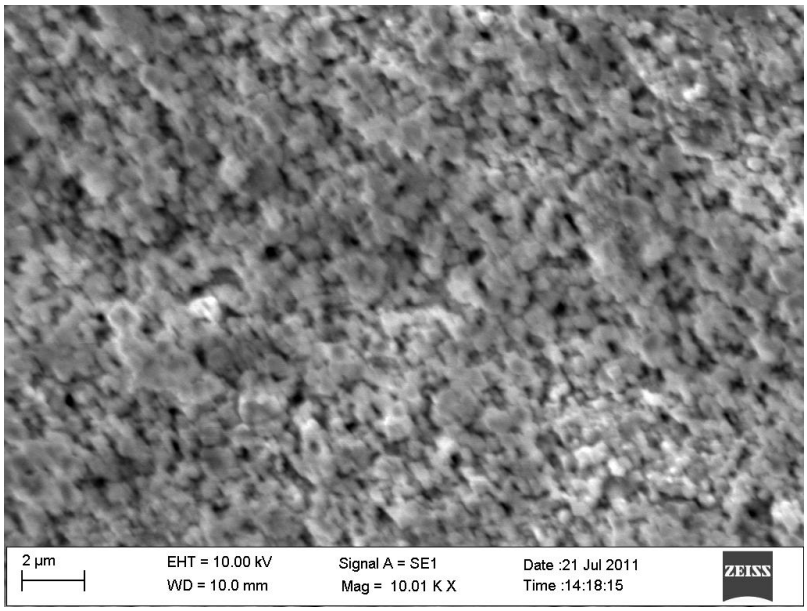

Figure 7(a) & (b) : Variation of DC Conductivity

IV. Conclusion:-

In this paper we report the preparation of strontium stannate by Oxalate Co- precipitation method. We have found the single phase orthorhombic structure. The phase formation of the sample was confirmed according the good agreement between observed and calculated d-values. Experimental density of the sample is 91.2% for pure strontium Stannate. Values of ε' and tan δ is almost flat over wide range of temperature. Impedance and modulus analysis are used to analysis the electrical conductivity of the materials. Comparative AC & DC conductivity is presented. Fine grain size is must be good for sample.

References:

[1]. Azad A M, Hon N C. ,Characterization of $BaSnO_3$ based ceramics, Synthesis, Processing and microstructure development,[J].Journal of Alloys and compounds, 1998,270(12),95-106.
[2]. Gopal Reddy C V. Manorama S V. Rao V J. preparation and characterization of barium Stannate, application as liquefied petroleum gas sensor [J]. J Mater Sci. Material in electronics, 2001, 12(2), 137-142.
[3]. Cerda J, Arbiol J, Dezanneau G, et al. Perovskite type $BaSnO_3$ powder for high temperature gas sensor application [j]. Sensors and Actuators B,2002, 84(1),21-25.
[4]. Y. Shimizu, M Shimalukuro, H. Arai and T. Seiyama,,J. Electro chem. Soc.136 (1989)1206.
[5]. R.Wernicke , Ber. Dtsch. Keram,Gas.55(1978)356.
[6]. D, Chen,J. Ye, $SrSnO_3$ nano structures : synthesis characterization and photo catalytic properties , J. Chem. Mater. 19(2007)4585-4591.
[7]. O. M. Prakash, K.D. Mandal,C.C. Christopher, M.S. Sastry,D. J. Kumar, preparation and characterization of strontium stannates,$SrSnO_3$, Mater.Sci. Lett. 13(1994)1616-1617.
[8]. A.M. Azad,L. W. Shyan, P.T. Yen, Characterization of $BaSnO_3$- based ceramics, Synthesis, processing and micros structural development. Alloys Compound, 282 (1999)109-124.
[9]. A. M. Azad, N. C. Hon, Synthesis, processing and micros structural characterization of $CaSnO_3$ and $SrSnO_3$ Ceramics. Alloys compd. 270 (1998)95-106.
[10]. H. Mizoguchi, P.M. Woodward, C.H. park ,D.A. Keszler, Strong near infrared luminescence in $BaSnO_3$, J. Am. Chem. Soc. 126 (2004) 9796-9800.
[11]. M.G. Smith, J.B. Good enough ,A Manthiram, R.D. Taylor, W. Peng, C.W. Kimball, Tin and antimony valence states in BaSn0.85 Sb 0.15 O_3-d,J. Sol. State Chem.98(1992)181-186
[12]. N. Sharma, K.M. Shaju, G.V. Subba Rao, B.V.R. Chowdari, Anodic behaviour and XPS of ternary tin oxides, J. Power Sources 139 (2005) 250–260.
[13]. M. Bao, W. Li, P.J. Zhu, Study on the dielectric properties of oxide-doped $Ba(Ti,Sn)O_3$ Ceramics prepared from ultrafine powder, Mater. Sci. 28 (1993)6617–6621.
[14]. M. Leoni, M. Viviani, P. Nanni, V. J. Buscaglia, Low-temperature aqueous synthesis (LTAS) of ceramic powders with perovskite structure, Mater. Sci. Lett. 15 (1996) 1302–1304.
[15]. C.P. U dawatte, M. Kakihana, M. Yoshimura, Low-temperature synthesis of pure $BaSnO_3$and the $(Ba1-x)SrxSnO_3$ solid-solution by the polymerize complex method, Sol. State Ionics 128 (2000) 217–226

Rakesh Kumar Kurre. "Studies the various property of strontium stannate prepared by coprecipitation method." *IOSR Journal of Applied Physics (IOSR-JAP)*, 15(2), 2023, pp. 21-27.